Angewandte Chemie
Eine Zeitschrift der Gesellschaft Deutscher Chemiker

Supporting Information

Chiral Selectivity of Secondary Nucleation in Amyloid Fibril Propagation

Mattias Törnquist and Sara Linse**

anie_202108648_sm_miscellaneous_information.pdf

Supplementary Material

This PDF file includes:

Materials and Methods
Supplementary Results
Figs. S1 to S7
Captions for Data S1

Other Supplementary Materials for this manuscript include the following:

Data S1

Materials and Methods

Materials:

All chemicals were of analytical grade. ThT was from CalBiochem and prepared as a 2 mM stock, filtered through 200 nm filter and concentration determined after filtration using UV absorbance of diluted samples. The synthesis and purification of two peptides with amino acid sequence FAEDVGSNKGAIIGL and non-capped termini, comprising residues 20-34 of Aβ with all-L and all-D amino acid residues, respectively, was purchased (GenScript, Piscataway, New Jersey). The L-Aβ20-34 and D-Aβ20-34 peptides were delivered as lyophilized HCl salts at 99.4 % (L-Aβ20-34), and 99.7% (L-Aβ20-34) purity, and size exclusion chromatography on a Superdex 30 increase column (GE Healthcare) was used to remove remaining small molecules (Fig. S1). The synthesis and purification of two peptides comprising residues 20-29 of human islet amyloid polypeptide (IAPP(20-29)) with the sequence SNNFGAILSS and non-capped termini, with all L-amino acids or all D-amino acids, respectively, was also purchased (GenScript, Piscataway, New Jersey). The L-IAPP(20-29) and D-IAPP(20-29) peptides were delivered as lyophilized as HCl salts at 98.2 % (L-IAPP(20-29)) and 98.4 % (D-IAPP(20-29)) purity. We found that D-IAPP(20-29) was highly soluble in DMSO (above 20 mM), while L-IAPP(20-29) was only soluble to 2.5 mM in DMSO, indicating that the received L-IAPP(20-29) contained a significant amount of non-peptide impurities. These impurities we removed by dispersing 20 mg peptide in 5 mL of 100% acetonitrile by sonication followed by centrifugation for 1 min at 6500 x g and the supernatant was discarded. The pellet was sonicated a second time in 5 mL 100 % acetonitrile and the supernatant removed after centrifugation for 1 min at 6500 x g. The resulting peptide pellet was dissolved in DMSO at 40 mM. The purity of all four peptides was confirmed by mass spectrometry (Figure S6-S7).

Preparation of seeds:

L-Aβ20-34 and D-Aβ20-34 peptide were each dissolved at 5 mM in ice-cold experimental buffer (20 mM sodium phosphate, 0.2 mM EDTA, 0.02% NaN_3, pH 7.4), pH adjusted with NaOH from 7.0 to 7.4 and the solutions was filtered through 30 kDa filter (Startorius). 20 µM ThT was added from a concentrated stock (filtered through 200 nm filter).

L-IAPP(20-29) and D-IAPP(20-29) were diluted to 300 µM from the concentrated DMSO stocks into filtered and degassed buffer, 20 mM sodium phosphate, 0.2 mM EDTA, 0.15 M NaCl, 20 µM ThT, 0.02% NaN_3, pH 8.0.

Samples were placed in wells of PEG-ylated polystyrene plates (Corning 3881 half-area for L- and D-Aβ20-34 and Corning 3560 full area for L- and D-IAPP(20-29)). The aggregation was monitored by reading the ThT fluorescence through the bottom of the plate at 37ºC, at quiescent condition, in a plated reader (BMG Omega) with excitation and emission filters at 440 and 485 nm, respectively. The seeds were collected from the wells into low-binding tubes (Axygen) after reaching the plateau in ThT fluorescence and sonicated for 2 minutes in a sonicator bath. Bath sonication was used as an attempt to de-clump the seeds just before use; however, the extent of de-clumping and the amount of catalytic surface may not be constant between samples.

Aggregation kinetics:

L-Aβ20-34 and D-Aβ20-34 peptide were each dissolved at 5 mM in ice-cold experimental buffer (20 mM sodium phosphate, 0.2 mM EDTA, 0.02% NaN_3, pH 7.4), pH adjusted with NaOH from 7.0 to 7.4. Monomers were isolated using size exclusion chromatography in the same buffer, which also removes small molecule contaminants (Figure S1). The resulting 3 mM monomer solution was collected on ice and supplemented with 20 μM ThT from a concentrated stock. The samples were placed in wells of a PEG-ylated polystyrene plate (Corning 3881 for L-and D-Aβ20-34 and Corning 3560 for L- and D-IAPP(20-29)) containing either 0.3% seed (final seed concentration 10 μM in monomer equivalents) or the equivalent volume of buffer.

L-IAPP(20-29) and D-IAPP(20-29) were diluted to 120 μM from the concentrated DMSO stocks into filtered and degassed buffer, 20 mM sodium phosphate, 0.2 mM EDTA, 0.15 M NaCl, 20 μM ThT, 0.02% NaN_3, pH 8.0. The samples were placed in wells of a PEG-ylated polystyrene plate containing either 0.3% seed (final seed concentration 0.36 μM in monomer equivalents) or the equivalent volume of buffer.

The aggregation was monitored by reading the ThT fluorescence through the bottom of the plate at quiescent condition, 37ºC, in a plated reader (BMG Omega) with excitation and emission filters at 440 and 485 nm, respectively. We noted for both Aβ20-34 and amylin, a higher ThT fluorescence intensity for the D-peptides.

Aggregation kinetics for mechanistic study: Samples of freshly isolated L-Aβ20-34 monomer were prepared in 20 mM sodium phosphate, pH 7.4, 0.2 mM EDTA, 0.02% NaN3, 20 μM thioflavin T at multiple monomer concentrations, 1.72-4.8 mM, supplemented at time zero with 0.3% preformed fibril seed in low-binding tubes (Axygen) in an icebox. Samples were pipetted into wells of a 96 well plate (Corning 3881 PEG-ylated black polystyrene half area with transparent bottom). Aggregation was initiated by placing the plate in a plate reader (BMG Omega) thermostated at 37^0C and the fluorescence was measured through the bottom of the plate using an excitation filter at 440 nm and an emission filter at 480 nm.

Circular Dichroism Spectroscopy: Far-UV circular dichroism (CD) spectra were recorded between 185 and 250 nm in a 0.1 mm cuvette using a Jasco J-720 spectropolarimeter with a scan rate of 10 nm/in, data integration tome 8s, bandwidth 1 nm. data pitch 1 nm, 3 accumulations.

Atomic Force Microscopy: Fibril samples were diluted 1:10 in water and immediately deposited on freshly cleaved mica. The mica substrates were heated to 70°C to rapidly dry the sample. Imaged on a AFM – Park XE 100 (Park Systems) in intermittent (non-contact) mode using a PointProbe® Plus probe (Park Systems) with a frequency of ~330kHz, and a force constant of 42 N/m.

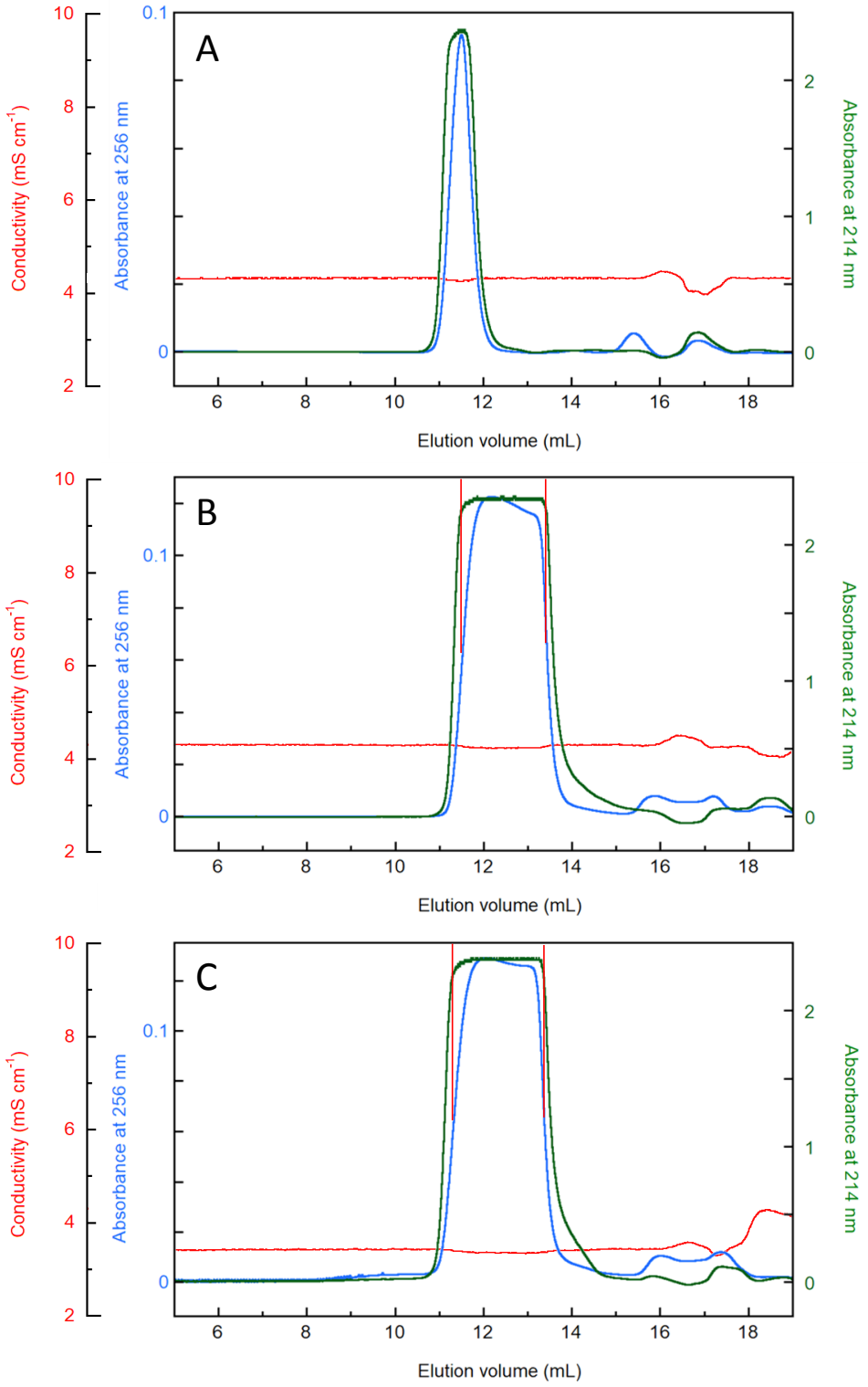

Figure S1. Size exclusion chromatography. SEC was performed in 20 mM sodium phosphate, 0.2 mM EDTA, 0.02% NaN_3, pH 7.4 using a Superdex 30 increase column at a flow rate of 0.7 mL/min. **A)** Analytical test SEC for L-Aβ20-34. **B**) Preparative SEC of L-Aβ20-34. **C**) Preparative SEC of D-Aβ20-34. Samples for kinetics were collected between the vertical lines.

Supplementary Results

The data obtained at 1.84-4.8 mM initial monomer concentrations with 0.3% seed were normalized and analyzed using the Amylofit platform (38). Data at 1.72 mM were excluded since only two out of four replicates aggregated within 180 h.

For an initial analysis, the half time of each reaction was extracted as the time point at which the ThT fluorescence intensity is half-way in between the initial baseline and final plateau values. The half time versus initial monomer concentration (c) was fitted by a power function

$$\text{half-time} = A\, c^{\gamma}$$

yielding a scaling exponent of $\gamma = -3.6$ (Figure S3). This excludes a fragmentation-dominated mechanism, which would give a scaling exponent of -0.5 (36, 39), and implies that the nucleated reaction has a high reaction order with $n_c \approx -2\gamma = 7.2$, or $n_2 \approx -(2\gamma + 1) = 6.2$ depending on whether the reaction is dominated by primary or secondary nucleation, respectively.

We next attempted to fit the normalized aggregation data globally using a set of different models. The model that produces the best fit to the data is dominated by secondary nucleation of monomers on the fibril surface (Figure S4A). This model includes secondary nucleation (rate constant k_2 and reaction order n_2), elongation (rate constant k_+). The model also includes primary nucleation (rate constant k_n and reaction order n_c), however, the fit is not sensitive to the values of those parameters as long as k_n is kept to a very low value, meaning this process is insignificant in accordance with the use of 0.3% seeds in all solutions at time zero. The fit shown in Figure S3A is for $k_2 = 6 \cdot 10^{14}\ M^{-6.5}\ h^{-1}$, $n_2 = 6.5$ and $k_+ = 540\ M^{-1}\ h^{-1}$).

Other models are much inferior. A model that includes primary nucleation with fitted reaction order ($n_c = 8$), elongation and fragmentation (Figure S4B) gives a significantly worse fit (2.5-fold higher error-square sum) and does not reproduce the steepness of the data as well as does the secondary nucleation model. A model devoid of any secondary process, i.e. only primary nucleation with fitted reaction order and elongation performers poorly and cannot reproduce the data (Figure S4C).

In conclusion, the global analysis of the data implies that the Aβ20-34 peptide aggregates via secondary nucleation of monomers on the fibril surface.

2.3 Solubility

The CD spectra observed after aggregation was completed for 3 mM samples of L and D peptide show a mixture of ß-sheet and random-coil signal, which implies that the solubility of the peptide is relatively high, with solubility referring to the monomer concentration in equilibrium with fibrils at the end of the reaction. Indeed, the spectra are compatible with an overlay of close to equal proportions of monomer and fibril spectra, suggesting that the solubility is roughly 1.5 mM. The lack of reproducible aggregation within 180 h for samples with concentration below 1.7 mM corroborates this estimate.

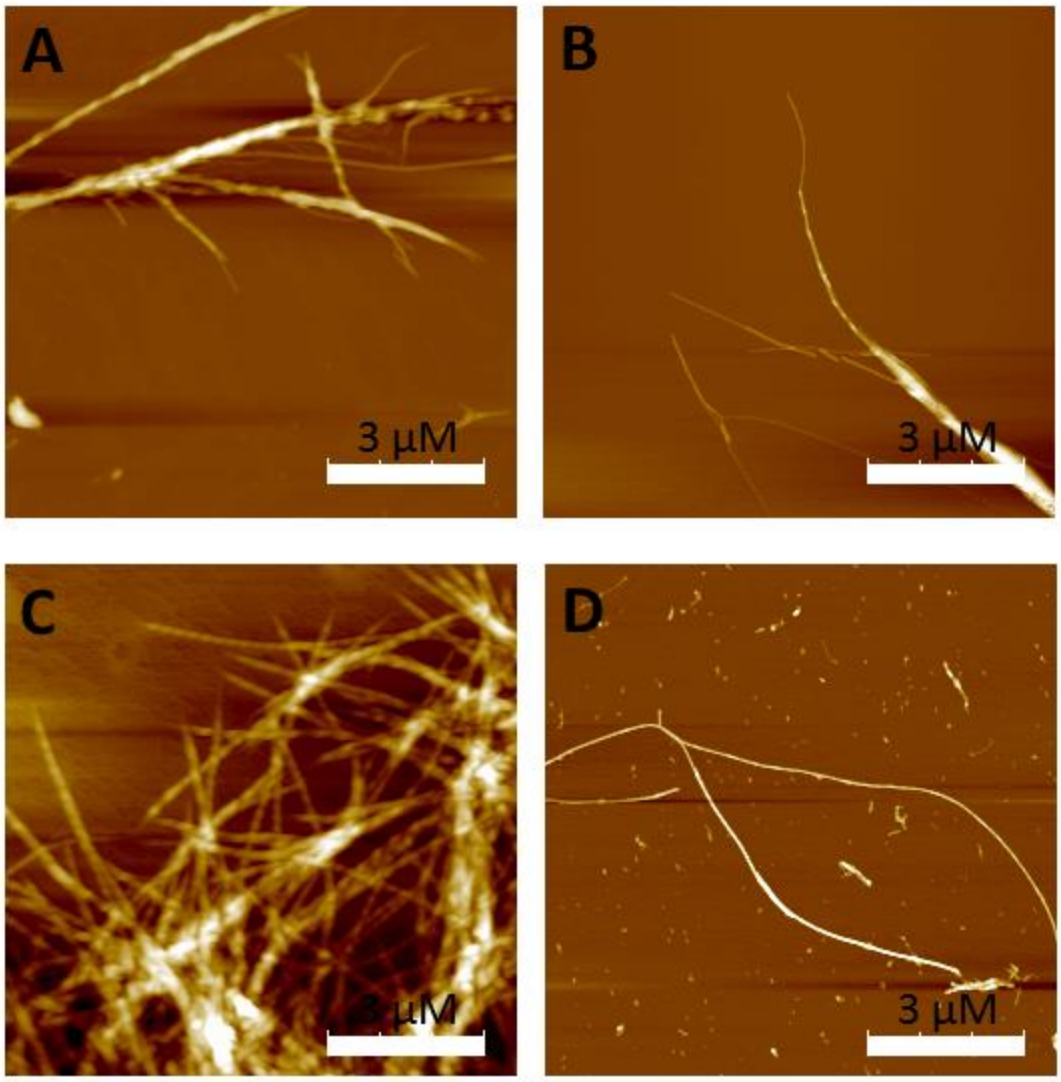

Figure S2. AFM topography images of fibrils made from L-Aβ20-34 (A, B) and D-Aβ20-34 (C, D).

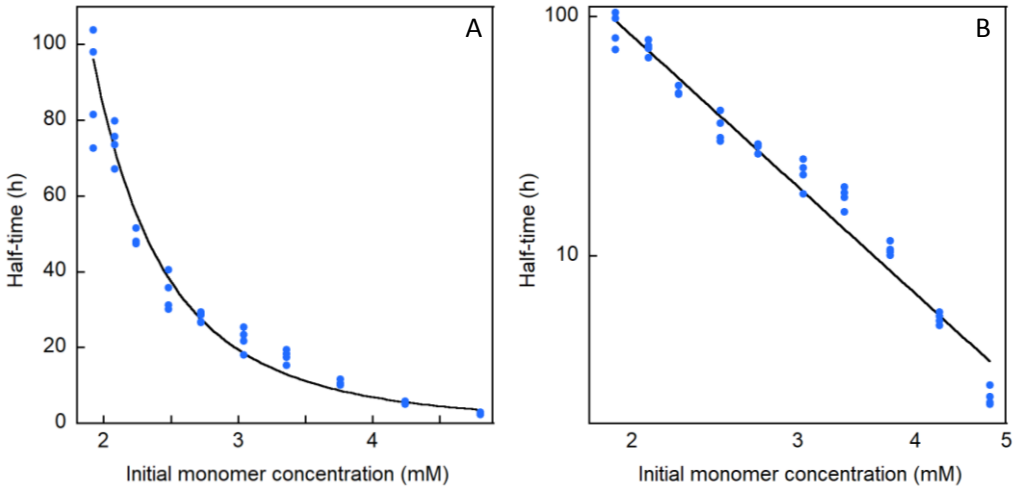

Figure S3. Scaling exponent. Half time of aggregation for L-Aβ20-34 as a function of initial monomer concentration, four replicates, plotted with **A**) linear and **B**) logarithmic axes. The solid line is a fit to the data points using a power function with a scaling exponent $\gamma = -3.6$.

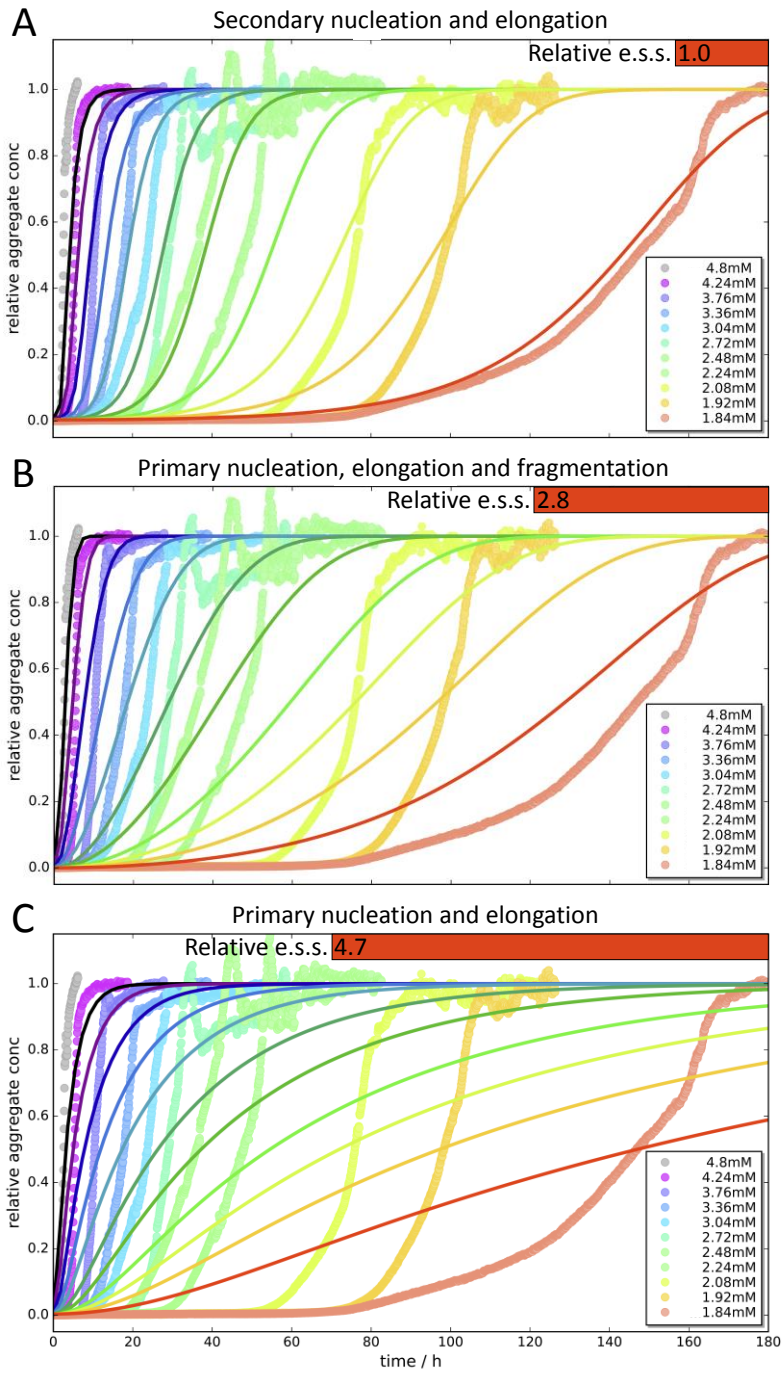

Figure S4. Global kinetic analysis. Normalized aggregation kinetics data starting from a series of samples with varying monomer concentration (ranging from 1.84-4.8 as indicated in the figure legend) and 0.3 % seed (concentration given in monomer concentration units). The closest to average of four replicates of each concentration is shown and the solid lines show the global fits of model with **A**) secondary nucleation and elongation (relative error square sum (e.s.s.) = 1.0, indicated by red bar), **B**) primary nucleation, elongation and fragmentation (relative e.s.s. = 2.8), **C**) primary nucleation, elongation and fragmentation (relative e.s.s. = 4.7).

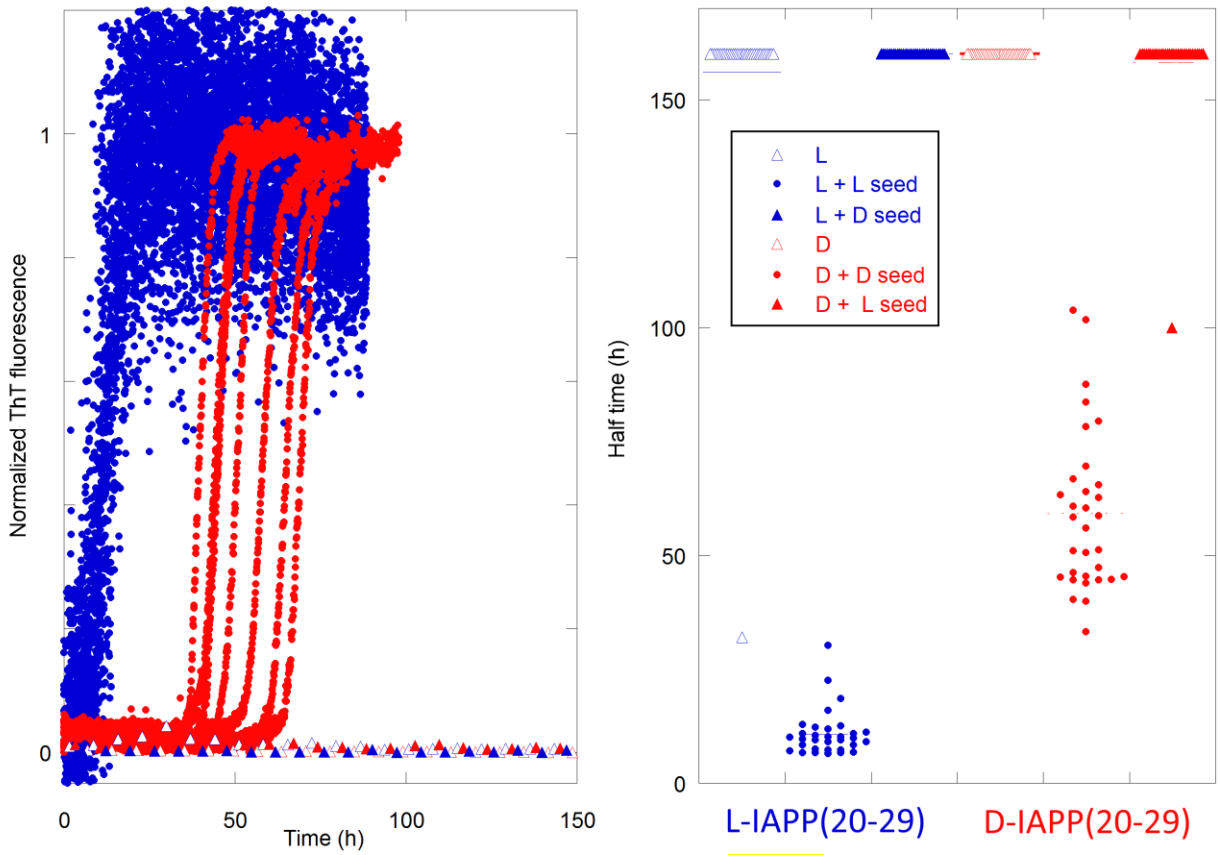

Figure S5. Self- and cross-seeded aggregation of IAPP(20-29). Aggregation kinetics for 120 µM monomer with or without 0.36 µM seed of the same or opposite chirality. **A**) Normalized ThT fluorescence for reactions starting at time zero from L monomer (open blue triangles), L monomer plus L seed (blue dot), L monomer plus D seed (filled blue triangles), D monomer (open red triangles), D monomer plus D seed (red dot), D monomer plus L seed (filled red triangles). Examples of curves are shown. **B**) Half-time of aggregation, defined as the point in time where the normalized ThT intensity is 0.5, extracted from all repeats for the self-seeded cases (L+L seed and D+D seed). Only one example of aggregation was observed for the non-seeded L case and one for the D + L seed case. None of the other cross- or non-seeded samples aggregated during the studied time course of 150+ hours. L refers to L-IAPP(20-29) peptide and D refers to D-IAPP(20-29) peptide.

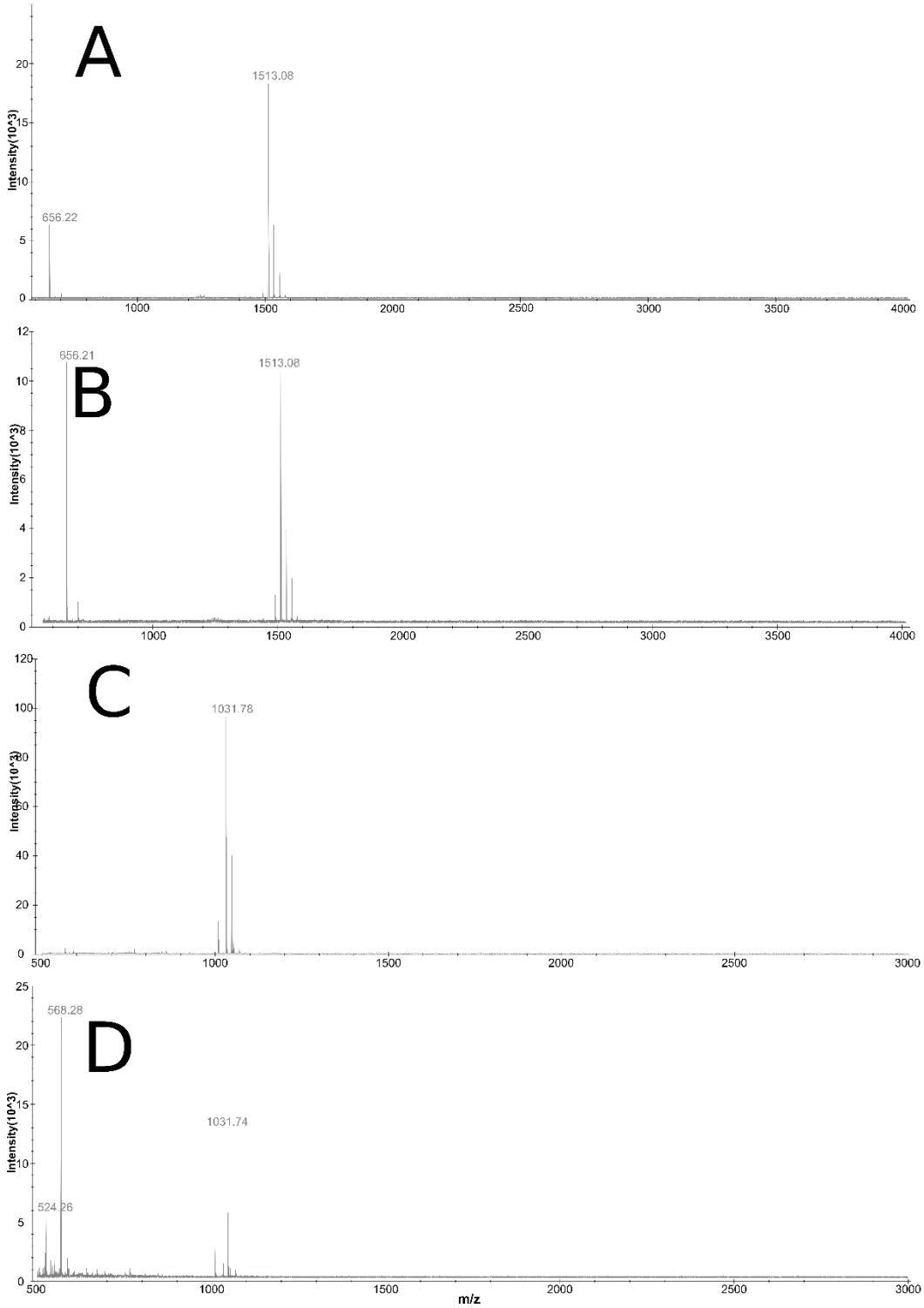

Figure S6. Mass spectrometry analysis. A) L-Aβ(20-34), **B)** D-Aβ(20-34) C**)** L-IAPP(20-29) **D)** D-IAPP(20-29)

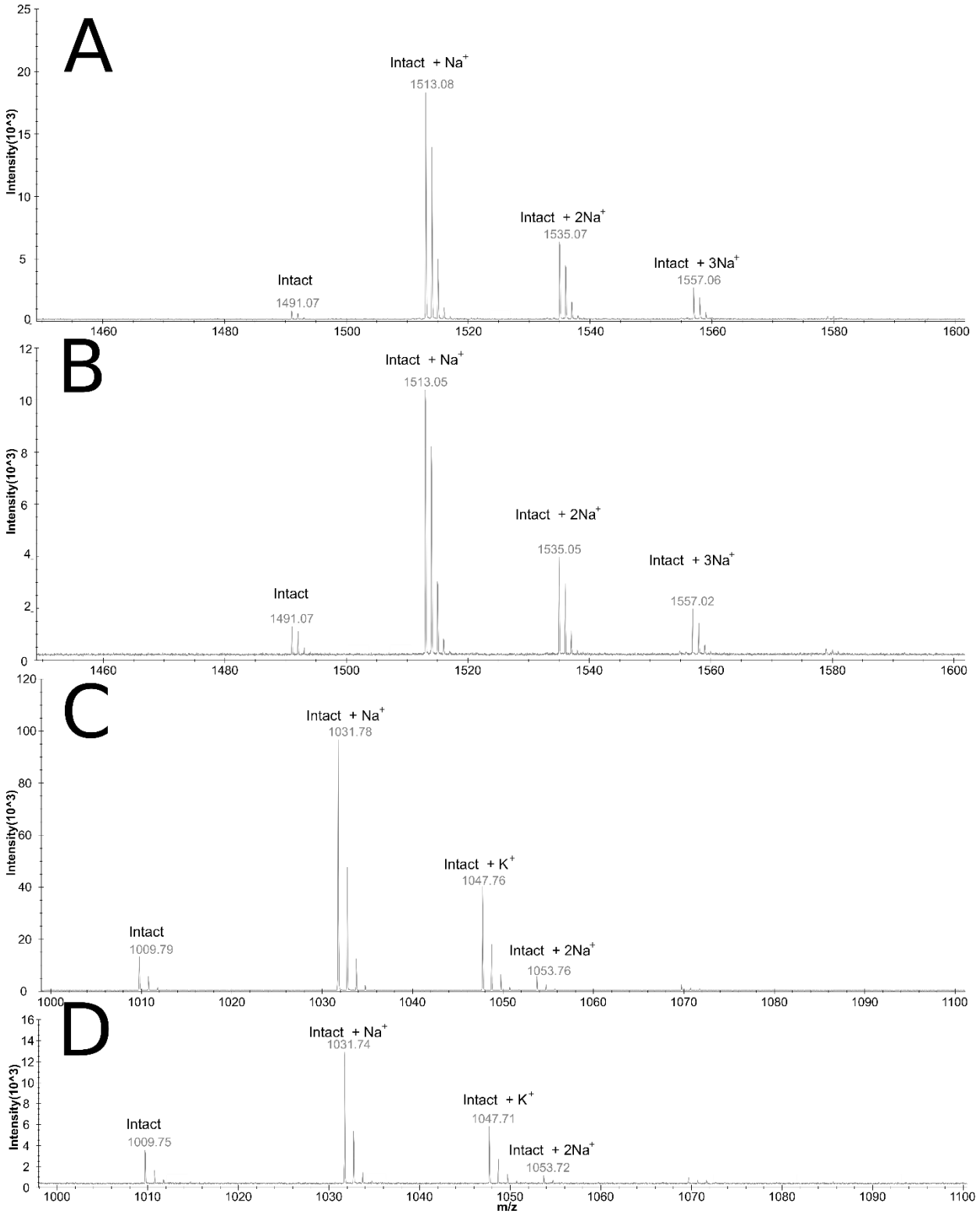

Figure S7. Mass spectrometry close-up of peptide peaks. A) L-Aβ(20-34), **B)** D-Aβ(20-34) C**)** L-IAPP(20-29) **D)** D-IAPP(20-29)

Data S1. (separate file)

Raw data underlying figure 2. Tab "**D_seed traces**" contains the data points that form the traces for the aggregation of the D monomer with D seed (red traces). Tab "**L_seed traces**" contains the data points that form the traces for the aggregation of the L monomer with L seed (blue traces). Note that not all traces start at time zero. The tab "**t_half data**" contain the aggregation half times in hours for the self-seeded L- and D-peptides.